2014

HMGB1 Enhances Immune Suppression by Facilitating the Differentiation and Suppressive Activity of Myeloid-Derived Suppressor Cells

K. H. Parker

P. Sinha

L. A. Horn

V. K. Clements

H. Yang
Northwell Health

See next page for additional authors

Authors
K. H. Parker, P. Sinha, L. A. Horn, V. K. Clements, H. Yang, J. H. Li, K. J. Tracey, and S. Ostrand-Rosenberg

Published in final edited form as:
Cancer Res. 2014 October 15; 74(20): 5723–5733. doi:10.1158/0008-5472.CAN-13-2347.

HMGB1 enhances immune suppression by facilitating the differentiation and suppressive activity of myeloid-derived suppressor cells

Katherine Parker[1], **Pratima Sinha**[1], **Lucas A. Horn**[1], **Virginia K. Clements**[1], **Huan Yang**[2], **Jianhua Li**[2], **Kevin J. Tracey**[2], and **Suzanne Ostrand-Rosenberg**[1]

[1]Department of Biological Sciences, University of Maryland Baltimore County, Baltimore, MD

[2]Laboratory of Biomedical Science, The Feinstein Institute for Medical Research, Manhasset, NY

Abstract

Chronic inflammation often precedes malignant transformation and later drives tumor progression. Likewise, subversion of the immune system plays a role in tumor progression, with tumoral immune escape now well recognized as a crucial hallmark of cancer. Myeloid-derived suppressor cells (MDSC) are elevated in most individuals with cancer, where their accumulation and suppressive activity are driven by inflammation. Thus, MDSC may define an element of the pathogenic inflammatory processes that driven immune escape. The secreted alarmin HMGB1 is a pro-inflammatory partner, inducer and chaperone for many pro-inflammatory molecules that MDSC development. Therefore, in this study we examined HMGB1 as a potential regulator of MDSC. In murine tumor systems, HMGB1 was ubiquitous in the tumor microenvironment, activating the NF-κB signal transduction pathway in MDSC and regulating their quantity and quality. We found that HMGB1 foments the development of MDSC from bone marrow progenitor cells, contributing to their ability to suppress antigen-driven activation of CD4+ and CD8+ T cells. Further, HMGB1 increased MDSC-mediated production of IL-10, enhanced crosstalk between MDSC and macrophages and facilitated the ability of MDSC to down-regulate expression of the naive T cell homing receptor L-selectin. Overall, our results revealed a pivotal role for HMGB1 in the development and cancerous contributions of MDSC in cancer patients.

Keywords

tumor immunity; inflammation & cancer; MDSC

Introduction

Anti-tumor immunity and immunotherapies that activate innate and/or adaptive immunity have potential for the prevention and/or treatment of primary and metastatic cancers. However, immunotherapies are frequently ineffective because cancer patients contain

Corresponding Author: S. Ostrand-Rosenberg, Department of Biological Sciences, University of Maryland Baltimore County, 1000 Hilltop Circle, Baltimore, MD 21250; phone: 410 455-2237; FAX: 410 455-3875; srosenbe@umbc.edu.

Disclosure of Potential Conflicts of Interest: The authors have no conflicts of interest.

immunosuppressive cells. Myeloid-derived suppressor cells (MDSC) (1) are present in virtually all patients with solid tumors and are major contributors to immune suppression. They facilitate tumor progression through multiple immune mechanisms including the inhibition of T and NK cell activation (2), polarization of immunity towards a tumor-promoting type 2 phenotype through their production of IL-10 (3), and by perturbing the trafficking of naïve T cells by down-regulating L-selectin (4). MDSC also use non-immune mechanisms to enhance tumor growth. They produce VEGF and matrix metalloproteases that promote tumor vascularization (5) as well as invasion and metastasis (6).

Chronic inflammation has long been associated with tumor onset and progression (7). The role of chronic inflammation was originally attributed to its ability to foster genetic mutations, enhance tumor cell proliferation and survival, and promote metastases. Chronic inflammation also facilitates malignancy by inducing the accumulation and increasing the potency of MDSC, which prevent adaptive and innate immunity from delaying tumor progression (8). Multiple redundant pro-inflammatory molecules drive MDSC. Since the Damage Associated Molecular Pattern molecule (DAMP) and alarmin High Mobility Group Box Protein I (HMGB1) is pro-inflammatory and is a binding partner, inducer, and/or chaperone for many of the pro-inflammatory molecules that drive MDSC (9), we have studied HMGB1 as a potential regulator of MDSC. HMGB1 was originally identified as a DNA binding protein in the nucleus. It performs multiple functions within the nucleus including changing the conformation of DNA to allow for the binding of regulatory proteins, facilitating the integration of transposons into DNA, and stabilizing nucleosome formation (10). Its role as a secreted protein and an immune modulator has only been recognized within the past 15 years (11).

We now report that in addition to many other cells, MDSC release HMGB1 and that HMGB1 activates MDSC through NF-κB and facilitates several immune suppressive mechanisms used by MDSC to inhibit anti-tumor immunity. HMGB1 drives the differentiation of MDSC from bone marrow progenitor cells, enhances crosstalk between MDSC and macrophages by increasing MDSC production of IL-10, and reduces the expression of L-selectin on circulating T cells. Collectively, these results suggest that HMGB1 contributes to immune suppression by inducing and activating MDSC.

Materials and Methods

Mice

BALB/c, C57BL/6, BALB/c IL-10$^{-/-}$, BALB/c TLR4$^{-/-}$, BALB/c DO11.10 (TCR-transgenic for the αβ-TCR specific for OVA peptide 323-339 restricted by I-A^{d}) and BALB/c clone 4 TCR-transgenic (αβ-TCR specific for influenza hemagglutinin 518-526 restricted by H-2K^{d}) mice were from The Jackson Laboratory (Bar Harbor, ME) and/or bred in the UMBC animal facility. Mice <6 months of age were used for all experiments. All animal procedures were approved by the UMBC IACUC.

Reagents and antibodies

Heparin sodium salt (grade IA) and ethyl pyruvate were from Sigma-Aldrich. Glycyrrhizin (ammonium salt) was from Calbiochem. Recombinant mouse IL-6 and GMCSF were from Biolegend. Recombinant mouse IFN-γ, HMGB1, and TNFα were from R&D Systems. Recombinant LPS was from Difco. mAbs Gr1-APC-Cy7, Gr1-APC (RB6-8C5), CD45-PE (30-F11), CD8-FITC (53-6.7), CD4-PE (L3T4/GK1.5), CD3-PE-Cy7 (145-2C11), CD11b-PE (M1/70), CD11c-FITC (HL3), CD45R-B220-PE (RA3-6B2), CD62L-APC (MEL14), c-kit-PE (CD117; ACK45), iNOS, arginase, rat IgG2b isotype, and annexin V were from BD Biosciences. CD11b-PacB (M1/70), F4/80-PE (BM8), F4/80-PacB (BM8), rat IgG1a-APC (RTK2758), and CD16/32 (93) were from BioLegend. CD45-TxR (MCD4517) was from Invitrogen. Anti-mouse ADAM17 mAb was from Abcam (ab2051). Secondary for ADAM17 antibody (goat-anti-rabbit; 554020) was from BD Biosciences. Anti-CD3 was from Dako (clone F7.2.38). Recombinant A Box (12, 13) and 2G7 (14) were produced as described.

Tumor inoculations, tumor measurements, 2G7, and A box treatment

C57BL/6 mice were inoculated s.c. in the flank with 5×10^5 MC38 colon carcinoma cells, 1×10^6 B78H1 melanoma cells, or 1×10^6 AT3 mammary carcinoma cells (15). BALB/c mice were inoculated in the abdominal mammary fat pad with 7×10^3 4T1 mammary carcinoma cells or s.c. with 1 x 10^6 CT26 colon carcinoma cells. With the exception of AT3, which was obtained from Dr. S. Abrams (Roswell Park Cancer Center) ~5 years ago, all tumor cell lines have been in the authors' laboratory for >15 years. Cell lines are routinely checked for mycoplasma and early freeze-downs are preferentially used. Recombinant A box (300μg/100 μl/mouse), vehicle (PBS), 2G7 mAb (5μg/200μl/mouse), or control IgG2b antibody (MOPC 195; 5μg/200μl/mouse; Sigma Aldrich) were administered intraperitoneally 3x/week starting when tumors were first palpable (day 7-9 post inoculation). Tumors were measured in two perpendicular diameters every 2-3 days. Tumor volume = πr^2 where r = (diameter 1 + diameter 2)/4. Immunohistochemistry for tumor-infiltrating T cells was performed by CD3 staining of O.C.T. embedded tumors.

Tumor, MDSC, and macrophage supernatants; MEF cell lysates

4T1, CT26, B78H1, MC38, and AT3 tumor cells were cultured at 5×10^6 cells/ml in 6 well plates in serum-free HL-1 medium at 37°C, 5% CO_2. MDSC and thioglycolate-elicited macrophages were similarly cultured except some wells contained 100ng/ml LPS. Supernatants were harvested after 18 hours and concentrated 10x using 10kDa Centricon filters (Millipore). Excised tumors were minced into small pieces using scissors, and placed in 10ml of serum-free HL-1 media containing 0.8μg/ml DNase. Tumor chunks were then dissociated into single cell suspensions using a GentleMACS Dissociator equipped with a GentleMACS C tube and program m_tumor 01.01 (Milltenyi Biotec). Dissociated material, including medium, was then plated in 10cm dishes and incubated at 37°C, 5% CO_2 for 18 hours, after which the supernatants were collected and concentrated to 2ml using 10kDa Centricon filters. Wild type and HMGB1-knocked out MEF cells (16) were lysed in 300μl of M-Per buffer Mammalian Protein Extraction Reagent (Thermo Scientific) using a GentleMACS fitted with an M tube and program protein 01.01. Lysates were centrifuged at

10°C and 650g for 5 minutes, and the supernatants removed and centrifuged at 10°C and 160g for 15 min. Protein concentration of the supernatants was determined at 280 absorbance.

Blood MDSC

Mice were bled from the submandibular vein into 1ml of PBS containing 0.008% heparin. RBC were removed by Gey's treatment (17). The remaining white blood cells were stained for Gr1 and CD11b and analyzed by flow cytometry. White blood cells that were >90% $Gr1^{+}CD11b^{+}$ were used in experiments.

MDSC- macrophage co-cultures

Peritoneal macrophage (>80%$CD11b^{+}F4/80^{+}$ cells) and MDSC co-cultures were performed as described (3). Briefly, cells were plated at 7.5×10^{5} MDSC and 7.5×10^{5} macrophages/well in 500ul of DMEM with 5% FBS, 100 ng/ml LPS, and 20 U/ml IFN-γ in 24 well plates. Co-cultures were incubated at 37°C, 5% CO_2 for 16-18 hrs. Supernatants were stored at −80°C until analyzed by ELISA.

Cytokine detection

IL-10, IL-6, IL-12, and IL-1β were measured by ELISA according to the manufacturer's protocol (R&D Systems). Plates were read at 450 nm using a Bio-Tek synergy microplate reader. Data are the mean ± SD of triplicate wells.

MDSC generation from bone marrow cells

MDSC were generated (18) with the following adaptations: Bone marrow was flushed aseptically from femurs with RPMI medium using a syringe fitted with a 27g needle. RBC were lysed with Gey's solution. Resulting cells were cultured at 37°C, 5% CO_2 at 4.2 x 10^{5} cells/2ml in 6 well plates containing RPMI medium supplemented with 10% FCS, 40 ng/ml IL-6 and 40 ng/ml GM-CSF. After four days of culture, percent decrease in $Gr1^{mid}CD11b^{+}$ cells was determined ($Gr1^{mid}CD11b^{+}$ cells = 100% [(number of vehicle-treated cells – number of inhibitor treated cells)/(number of vehicle-treated cells)]. Absolute number of cells = (total number of cells) x % of a given cell type as determined by flow cytometry.

T cell activation assays

T cell activation assays were performed as described (17). Briefly, splenocytes and irradiated (2500 Rad) 4T1-induced MDSC or bone marrow generated MDSC were co-cultured in 96 well plates at 10^{5} cells/200μl/well of HL-1 media containing 1% penicillin, 1% streptomycin, 1% Glutamax, and 5 x 10^{-5} M β-mercaptoethanol. 14uM $OVA_{323-339}$ peptide or 28 μM $HA_{518-526}$ peptide was included for DO11.10 and clone 4 cells, respectively. Wells were pulsed with 1μCi of [^{3}H] thymidine/well on day 3, and 18 hours later the cells were harvested. Data are expressed as cpm ± SD of triplicate cultures. Hydrogen peroxide levels were measured as described (19).

HMGB1 western blots and ELISA

50 μl of equivalent quantities of concentrated supernatants of cultured tumor cells, in vivo grown tumors, MDSC, macrophages, or 60ug of MEF cell lysates were mixed with 10 μl or the appropriate amount of 6x sample buffer and electrophoresed on 12% SDS-PAGE gels in SDS running buffer (BioRad) at 150 volts for 1 hour, and transferred overnight in transfer buffer (BioRad) at 30 volts to PVDF membranes (GE Healthcare). Membranes were blocked with 5% milk in TBST. HMGB1 was detected with anti-HMGB1 antibody (Epitomics) (5ng/ml in 10ml of 2.5% milk/TBST) followed by goat-anti-rabbit-HRP (Millipore) (40ng/ml in 10ml of 2.5% milk/TBST). Protein was visualized using an HRP detection kit (Denville Scientific, Inc). HMGB1 levels were measured by ELISA according to the manufacturer's directions (IBL International, Hamburg, Germany).

Flow cytometry

Cells were labeled and analyzed by flow cytometry for cell surface molecules as described (17). For bone marrow experiments, cells were first stained using the LIVE/DEAD fixable yellow dead cell stain kit (Invitrogen) per the manufacture's protocol, followed by staining for cell surface markers with antibodies diluted in PBS/ 2% FCS (HyClone). For NF-κB staining of MDSC, 3×10^6–5×10^6 leukocytes/ml RPMI were incubated with/without 50 ng/ml HMGB1 for 15 minutes at 37°C, fixed and permeabilized and then stained with rabbit mAb phospho-NF-κB p65 (Ser536; clone 93H1) and goat-anti-rabbit $(Fab')_2$-AlexaFluor 647 (Cell Signaling, Inc.) according to the manufacturer's protocol, followed by staining for Gr1 and CD11b. Peritoneal macrophages (5×10^6/5 ml DMEM) were similarly stained, except they were rested for 2 hrs at 37°C before stimulation with 20ng/ml TNFα or 100ug/ml LPS, and subsequently incubated with Fc block (CD16/32) for 15 min., followed by staining with NF-κB, CD11b, and F4/80 mAbs. For ADAM17 staining, 3×10^6–5×10^6 leukocytes were incubated with or without HMGB1 (50 ng/ml) or ethyl pyruvate (10mM) for zero, two, and four hours and stained with mAb to ADAM17. For tumor-infiltrating MDSC, solid tumors were prepared as they were for tumor supernatants, except collagenase (300 U/ml) was included in the dissociation medium, and the resulting cells were centrifuged through ficoll to remove dead cells. Samples were run on a Cyan ADP flow cytometer and analyzed using Summit Software (Beckman/Coulter).

Statistical methods

Statistical analysis of tumor growth rate was conducted utilizing the compare Growth Curves function of the Statmod software package (http://bioinf.wehi.edu.au/software/compareCurves). Student's *t* test was used to determine statistical significance between two sets of data. Single-factor ANOVA was used to determine statistical significance between groups of data.

Results

HMGB1 is ubiquitously present in the tumor microenvironment and activates MDSC via the NF-κB pathway

If HMGB1 is associated with the induction of MDSC, then HMGB1 will be present in the tumor microenvironment. To test this hypothesis BALB/c-derived 4T1 mammary carcinoma and CT26 colon carcinoma cells, and C57BL/6-derived B78H1 melanoma, MC38 colon carcinoma, and PyMT-MMTV-derived AT3 mammary carcinoma cells were cultured in serum free-media, and the supernatants assessed by western blot for HMGB1. Whole cell lysates of wild type MEF cells and their HMGB1-knocked out counterparts served as positive and negative controls, respectively. All tumors constitutively secreted HMGB1 (**Fig. 1 *A***). Secretion of HMGB1 was confirmed and quantified by ELISA (**Supplementary Table 1**).

Since MDSC are driven by inflammation and themselves produce pro-inflammatory mediators (8, 20), we tested MDSC for secretion of HMGB1. MDSC generated in 4T1 tumor-bearing BALB/c mice were harvested from the blood, stained for Gr1 and CD11b, and assessed for their ability to suppress T cell activation (**Fig. 1*B***). Greater than 90% of the blood leukocytes were $CD11b^{+}Gr1^{+}$ and they were suppressive. We then tested MDSC for their ability to secrete HMGB1 by culturing them overnight and assaying the supernatant for HMGB1 by western blot and ELISA (**Fig. 1*C***, **Supplementary Table 1**). Macrophages are established producers of HMGB1 (11) and LPS is reported to increase their secretion of HMGB1 (21). To determine if LPS similarly affects MDSC, MDSC were cultured with and without LPS. Both LPS-treated and untreated MDSC produced more HMGB1 than equivalent numbers of LPS-treated macrophages, demonstrating that MDSC constitutively secrete HMGB1.

To determine if HMGB1 is present in vivo within the tumor microenvironment, 4T1, CT26, B78H1, MC38, and AT3 tumors of BALB/c and C57BL/6 tumor-bearing mice were measured, and then excised and weighed. Explanted tumors were then dissociated into single cell suspensions without disrupting cell integrity, and incubated in serum-free medium. The resulting supernatants were assessed by western blot and ELISA for HMGB1 (**Fig. 1*C* right-hand 5 lanes, Supplementary Table 1**). All excised tumors released HMGB1; however, the quantity of HMGB1 released did not directly correlate with tumor burden. Since different types of tumors contain different quantities of HMGB1-producing cells and necrotic cells (i.e. tumor cells, macrophages, MDSC, etc.), it is not unexpected that HMGB1 levels are not proportional to tumor mass.

HMGB1 binds to multiple receptors including two receptors that are expressed by MDSC: TLR4 (22) and Receptor for Advanced Glycation Endproducts (RAGE) (23). Signaling through both of these receptors converges on the NF-κB signal transduction pathway. To determine if HMGB1 activates MDSC, leukocytes from the blood of tumor-free BALB/c mice were cultured with or without HMGB1, subsequently stained for phosphorylated NF-κB (pNF-κB), and the $Gr1^{+}CD11b^{+}$ cells gated and analyzed for pNF-κB (**Fig. 1*D***). HMGB1-treatment caused phosphorylation of NF-κB.

To confirm the specificity of the pNF-κB staining, macrophages from either $TLR4^{+/+}$ or $TLR4^{-/-}$ mice were treated with either LPS or TNFα. If the pNF-κB mAb is specific, then TNFα will activate NF-κB in both $TLR4^{+/+}$ and $TLR4^{-/-}$ cells since it acts via the TNFα receptor. In contrast, NF-κB will only be activated by LPS in $TLR4^{+/+}$ cells, since LPS activates NF-κB via TLR4. TNFα activated NF-κB in both $TLR4^{+/+}$ and $TLR4^{-/-}$ cells, while LPS activated NF-κB in $TLR4^{+/+}$, but not $TLR4^{-/-}$ cells, confirming the specificity of the pNF-κB mAb (**Supplementary Fig. S1**).

These data indicate that HMGB1 is ubiquitously present in vivo in the tumor microenvironment, multiple cell populations within the tumor microenvironment produce HMGB1, MDSC contribute to the production of HMGB1, and HMGB1 activates the NF-κB signal transduction pathway in MDSC.

HMGB1 drives the differentiation of MDSC from bone marrow progenitor cells

Since the differentiation, accumulation, and function of MDSC are driven by inflammation (8, 20, 24, 25), HMGB1 may regulate MDSC by either controlling their accumulation and/or affecting their functional activities. To assess if HMGB1 affects MDSC differentiation, bone marrow cells from the femurs of healthy BALB/c mice were cultured under conditions that drive the differentiation of MDSC (18). The HMGB1 inhibitors ethyl pyruvate and glycyrrhizin were included in some cultures. Ethyl pyruvate prevents extracellular secretion of HMGB1 from activated monocytes and macrophages by blocking NF-κB signaling (26). Glycyrrhizin prevents the binding of extracellular HMGB1 by attaching to two distinct regions of HMGB1 (27). At the end of the four day culture period, the presence of HMGB1 was confirmed by western blot (**Fig. 2*A***) and quantified by ELISA (**Supplementary Table 1**), and the absolute number of $Gr1^{mid}CD11b^{+}$ cells was determined by cell counting and flow cytometry (**Fig. 2*B***). At the start of culture, 5.5×10^{4} cells were $Gr1^{mid}CD11b^{+}$. At the end of the culture period the vehicle control-treated cultures contained 1.6×10^{5} $Gr1^{mid}CD11b^{+}$ cells indicating that MDSC had expanded by almost 3 fold. Both HMGB1 inhibitors significantly reduced the absolute number of MDSC (**Fig. 2*C*, Supplementary Table 2**). The highest dose of glycyrrhizin reduced the number of $Gr1^{mid}CD11b^{+}$ cells by 82%, while ethyl pyruvate reduced the number by 80%. $Gr1^{+}CD11b^{+}$ MDSC induced under these conditions were just as suppressive as tumor-induced MDSC isolated from mice with 4T1 tumors (**Fig. 2D**). Glycyrrhizin and ethyl pyruvate also decreased the generation of DC ($CD11c^{+}$ cells, 43% and 67%, respectively) and macrophages ($F4/80^{+}CD11b^{+}$ cells, 66% and 68%, respectively), consistent with published reports showing that HMGB1 also drives the maturation of these cells (28). In contrast, B cells ($B220^{+}$ cells) and T cells ($CD3^{+}$ cells) were either not affected or only minimally decreased.

To determine if inhibition of HMGB1 reduces MDSC accumulation by inhibiting the proliferation of MDSC progenitor cells or by causing apoptosis of differentiated MDSC, bone marrow cells and matured MDSC were vehicle or ethyl pyruvate-treated and the levels of c-kit^{+} (CD117) progenitor cells and Annexin $V^{+}PI^{+}$ apoptotic cells were determined by flow cytometry (**Fig. 2E, Supplementary Fig. S2A**). Ethyl pyruvate reduced the level of progenitor cells but did not induce apoptosis as compared to vehicle treatment. These data

indicate that HMGB1 facilitates the expansion of myeloid cells, including MDSC, from bone marrow progenitor cells.

HMGB1 contributes to the ability of MDSC to suppress antigen-driven T cell activation

MDSC use multiple mechanisms to suppress anti-tumor immunity. Suppression of antigen-driven T cell activation was one of the first mechanisms identified (29, 30). To determine if HMGB1 impacts MDSC suppression of T cell activation, MDSC from 4T1 tumor-bearing BALB/c mice were tested for their ability to prevent the proliferation of transgenic $CD4^+$ (DO11.10) or $CD8^+$ (Clone 4) T cells activated with cognate peptides (**Fig. 3*A***). Increasing concentrations of the HMGB1 inhibitor ethyl pyruvate restored T cell activation in the presence of MDSC. Since ethyl pyruvate prevents signaling through NF-κB and T cell activation requires NF-κB signaling (31), transgenic T cells were treated with ethyl pyruvate to ascertain that these doses were not affecting T cell proliferation (**Fig. 3*B***). Ethyl pyruvate did not increase T cell activation in the absence of MDSC, demonstrating that the increase in T cell activation seen in fig. 3A is an effect of ethyl pyruvate on MDSC and not an effect on T cells.

To determine how ethyl pyruvate inhibits MDSC, control and ethyl pyruvate-treated MDSC were assayed by flow cytometry for their content of molecules that mediate T cell suppression (arginase, iNOS, and H_2O_2), and for its impact on MDSC viability. Ethyl pyruvate did not decrease arginase or iNOS levels or alter MDSC apoptosis levels (**Supplementary Fig. S2B, S2C**), but modestly reduced H_2O_2 levels (**Supplementary Fig. S2D**) as compared to vehicle-treated cells. In previous studies, another NF-κB inhibitor, Withaferin A, also reduced the suppressive potency of MDSC (19). These results suggest that HMGB1 contributes to MDSC-mediated T cell suppression by increasing their expression of H_2O_2.

HMGB1 increases MDSC production of IL-10 and MDSC-macrophage crosstalk

One of the mechanisms MDSC use to inhibit anti-tumor immunity is their production of IL-10. MDSC-produced IL-10 reduces macrophage production of IL-12, thereby skewing macrophages towards a type 2 tumor-promoting phenotype (3). Crosstalk between MDSC and macrophages increases MDSC production of IL-10, thereby contributing to MDSC suppression. MDSC-produced IL-10 also drives the differentiation and accumulation of T regulatory cells (32), further increasing immune suppression. To determine if HMGB1 drives MDSC production of IL-10 or MDSC-macrophage crosstalk with respect to IL-10, MDSC and macrophages were co-cultured with or without ethyl pyruvate and glycyrrhizin and IL-10 production was measured (**Fig. 4*A***). Both ethyl pyruvate and glycyrrhizin dose-dependently reduced the production of IL-10 by MDSC and by mixtures of MDSC plus macrophages. To ascertain that MDSC, rather than macrophages, are the producers of IL-10, macrophages and MDSC from IL-10-deficient BALB/c mice were used in conjunction with MDSC or macrophages, respectively, from wild type BALB/c mice (**Fig. 4*B***). Only marginal levels of IL-10 were detected in cultures containing $IL\text{-}10^{-/-}$ MDSC with wild type macrophages, demonstrating that MDSC are the cells producing the IL-10. The reduction of IL-10 is not due to reduced MDSC viability since ethyl pyruvate-treated MDSC cultured under the crosstalk conditions (with 5% serum) are more viable than vehicle-treated

MDSC (**Supplementary Fig. S2C**). These findings indicate that HMGB1 regulates MDSC production of IL-10 and macrophage-induced increases in MDSC production of IL-10.

MDSC also promote a type 2 immune response by down-regulating macrophage production of IL-12 (3) and IL-6 (unpublished). To determine if HMGB1 mediates either of these effects, MDSC and macrophages were co-cultured with or without ethyl pyruvate and glycyrrhizin and IL-12 and IL-6 were quantified by ELISA (**Fig. 5**). Ethyl pyruvate and glycyrrhizin reduced macrophage production of IL-12 and IL-6, and did not restore production of these cytokines in MDSC-macrophage co-cultures. IL-1β, a pro-inflammatory cytokine that is produced by MDSC and also drives the suppressive potency of MDSC (33, 34), was also assessed. Ethyl pyruvate and glycyrrhizin decreased MDSC production of IL-1β; however, HMGB1 inhibition restored IL-1β levels in co-cultures of MDSC and macrophages. These results indicate that HMGB1 regulates MDSC production of IL-1β during MDSC-macrophage crosstalk; however it is not involved in MDSC-mediated down-regulation of macrophage-produced IL-12 or IL-6.

Neutralization of HMGB1 delays tumor growth and reduces MDSC in tumor-bearing mice

HMGB1 includes two functional domains: the pro-inflammatory B Box and the anti-inflammatory A Box. The B Box is a RAGE agonist, while the A Box is a RAGE antagonist (13). Although the A Box is a competitor for the B Box, the B Box of HMGB1 is dominant in vivo (27). However, if administered in vivo as a recombinant protein, A Box neutralizes endogenous HMGB1 (14). To determine if A Box impacts tumor progression, BALB/c and C57BL/6 mice bearing 4T1 or MC38 tumor, respectively, were treated with A Box or vehicle control starting when the tumors were first palpable (approximate day 7-9 after tumor cell inoculation) (**Fig. 6*A***). In both strains, A Box delayed tumor progression, supporting the concept that HMGB1 facilitates tumor growth. 4T1 tumor cells were also knocked-down by shRNA for HMGB1 (4T1/575 cells) and their tumorigenicity compared to that of 4T1 cells transfected with an irrelevant shRNA (4T1/irrelevant) (**Supplementary Fig. S3*A***). The effect of HMGB1 on spontaneous metastatic disease was assessed by treating 4T1 tumor-bearing mice with glycyrrhizin and ethyl pyruvate and assessing the number of metastatic cells by clonogenic assay (35) (**Supplementary Fig. S3*B***). 4T1/575 tumor-bearing mice survived significantly longer than mice with 4T1/irrelevant cells supporting previously published work (36). Tumor-bearing mice treated with the inhibitors trended towards fewer metastatic cells; however, the values were not statistically significantly different. These results further confirm that HMGB1 enhances tumor progression.

To determine if HMGB1 drives MDSC accumulation in vivo, tumor-bearing mice were treated with a neutralizing HMGB1 mAb (2G7), and tumor-infiltrating MDSC and MDSC from the blood and spleen were compared to MDSC in vehicle-treated tumor-bearing mice. C57BL/6 mice were inoculated with the MC38 tumor on day 1 and 2G7 treatment was started on day 10-13. Mice were sacrificed at a late stage of disease when their primary tumors were approximately the same diameter, and total MDSC, monocytic MDSC, and granulocytic MDSC levels in the blood, spleen, and infiltrating the tumors were determined by flow cytometry (**Fig. 6B**). Total, monocytic, and granulocytic MDSC were reduced in the

spleens, blood, and tumors of 2G7-treated mice with the exception of tumor-infiltrating granulocytic MDSC. These decreases were not a secondary effect of reduced tumor size since, at the time of analysis, the 2G7-treated and control-treated mice had similar-sized primary tumors. MDSC were similarly reduced in the blood of A Box-treated tumor-bearing mice. These results indicate that in vivo, neutralization of HMGB1 reduces the accumulation of MDSC in tumor-bearing mice.

Tumors from the HMGB1 mAb-treated (2G7) and isotype control-treated mice of **Fig. 6** were assessed by immunohistochemistry for the presence of $CD3^+$ T cells (**Supplementary Fig. 4**). Both types of tumors contained few T cells; however, there was a trend towards more $CD3^+$ cells in the tumors of 2G7-treated mice.

HMGB1 down-regulates T cell expression of L-selectin

MDSC also impair T cell immunity by perturbing the homing of naive T cells to lymph nodes where they could become activated. To enter lymph nodes T cells must first be tethered via L-selectin (CD62L) to the walls of high endothelial venules (HEV) so they can extravasate from the bloodstream. Our previous in vitro studies showed that MDSC reduce T cell levels of L-selectin through their constitutive expression of ADAM17 (a disintegrin and metalloproteinase domain 17), an enzyme that cleaves the ectodomain of L-selectin (4). Subsequent in vivo vital imaging studies showed that T cells with reduced expression of L-selectin do not enter HEVs (J. Muhich, S. Ostrand-Rosenberg, S. Abrams, and S. Evans, unpublished). To determine if HMGB1 impacts MDSC-mediated down-regulation of T cell-expressed L-selectin, A Box and control-treated mice were sacrificed 29 days after tumor inoculation and circulating $CD45^+CD3^+CD4^+$ and $CD45^+CD3^+CD8^+$ T cells were analyzed for L-selectin by flow cytometry (**Fig. 7*A***). Circulating $CD4^+$ and $CD8^+$ T cells from tumor-free mice were controls for normal L-selectin expression. L-selectin was reduced in $CD4^+$ and $CD8^+$ T cells of tumor-bearing vehicle-treated mice, while A box-treatment partially restored L-selectin expression (**Fig. 7*B***). To confirm that HMGB1 acts on MDSC to reduce L-selectin, $Gr1^+CD11b^+$ cells from tumor-free and tumor-bearing mice were treated for zero, two, or four hours with HMGB1 or ethyl pyruvate, respectively. The cells were then stained with mAbs to Gr1, CD11b, and ADAM17, and the gated $Gr1^+CD11b^+$ cells were analyzed for plasma membrane expression of ADAM17 (**Fig. 7*C***). HMGB1-treated $Gr1^+CD11b^+$ cells from tumor-free mice expressed more ADAM17, while ethyl pyruvate-treated MDSC from tumor-bearing mice had less ADAM17, as compared to vehicle-treated cells. These observations indicate that plasma membrane ADAM17 turns-over on MDSC and that HMGB1 contributes to the down-regulation of L-selectin on T cells by sustaining MDSC expression of ADAM17.

Discussion

The DAMP and alarmin HMGB1 is released by many tumor cells, is elevated in the serum of many cancer patients (37), and is recognized as an enhancer of tumor progression by its direct action on tumor cells (9, 10, 28). The studies reported here identify MDSC, along with tumor cells and macrophages, as producers of HMGB1. The observed decrease in MDSC of tumor-bearing mice following treatment with HMGB1 inhibitors, combined with the in vitro

mechanistic studies demonstrate that HMGB1 (i) promotes the differentiation of MDSC from bone marrow progenitor cells; (ii) increases MDSC-macrophage crosstalk and MDSC production of IL-10; and (iii) increases MDSC-mediated down-regulation of L-selectin on naive T cells. These findings support the conclusion that HMGB1 contributes to the elevation and suppressive potency of MDSC in tumor-bearing mice, and identify a new pro-inflammatory mediator that regulates MDSC.

HMGB1 is likely to activate and drive MDSC because it induces, chaperones, and/or enhances the activity of several pro-inflammatory molecules that regulate MDSC. For example, IL-1β drives MDSC accumulation and T cell suppressive activity (33, 38) and is induced by HMGB1 (14). Complexes of HMGB1 and IL-1β have increased pro-inflammatory activity relative to either molecule alone (39). HMGB1 also enhances the pro-inflammatory activity of IL-6 (40), TNFα (14), and prostaglandin E2 (41), three other pro-inflammatory mediators that drive MDSC (24, 34, 42, 43). Although neutralization of HMGB1 significantly down-regulates MDSC suppressive activity, it does not globally neutralize MDSC, most likely because the multiple pro-inflammatory mediators that drive MDSC are redundant and can also be regulated by molecules other than HMGB1.

HMGB1 is known to facilitate tumor progression by co-opting other immune cells and by directly affecting tumor cell growth (9, 10, 28). It increases the accumulation of T regulatory cells and diverts type 1 T helper cells to a pro-tumor type 2 phenotype (36, 44). HMGB1 also acts directly on tumor cells to enhance tumor progression by binding to tumor cell-expressed RAGE. Many tumor cells express RAGE (45), and the binding of HMGB1 to RAGE promotes tumor cell autophagy, inhibits tumor cell apoptosis, and increases tumor cell invasiveness (46, 47). Collectively these effects produce an immune suppressive and pro-tumor environment. MDSC contribute to tumor growth through their immune suppressive mechanisms. However, their elimination may not be sufficient for tumor rejection, and active immunization of T cells and/or repolarization of macrophages to a M1-like phenotype may also be required (17). The studies reported here demonstrate that HMGB1 affects MDSC development and function. Since HMGB1 impacts tumor progression through multiple mechanisms that act on both tumor cells and immune cells, its effects on MDSC represent only one of its modes of action.

Paradoxically, under some conditions HMGB1 facilitates the activation of tumor-reactive T cells. HMGB1 facilitates dendritic cell maturation (48) and enhances DC-mediated antigen presentation during chemotherapy and radiotherapy (49). In contrast to the pro-tumor effects of HMGB1 which are thought to be transmitted through RAGE, the enhancement of DC function requires the release of HMGB1 by dead tumor cells and is mediated through DC-expressed TLR4. Whether the in vivo pro-tumor or anti-tumor effects of HMGB1 balance each other, or whether one dominates is unclear. However, the potential for HMGB1 to both inhibit and promote anti-tumor immunity makes it difficult to evaluate whether neutralization of HMGB1 will be beneficial or harmful.

The quantity of HMGB1 within different solid tumors differs significantly (**see Supplementary Table 1**). MDSC, macrophages, tumor-infiltrating cells, and tumor cells themselves all contribute to the amount of HMGB1 in the tumor microenvironment. Live

tumor cells secrete HMGB1, while necrotic tumor cells induced by suboptimal vascularization and hypoxia release nuclear HMGB1. Because the quantity of tumor-infiltrating cells and the extent of vascularization and hypoxia differ in different types of tumors, it is not unexpected that the quantity of HMGB1 within solid tumors does not correlate with tumor mass.

HMGB1 binds to both TLR4 and RAGE, and MDSC express both receptors (20, 50). TLR4 and RAGE signaling converges at NF-κB (9, 10, 28, 51), so that activation through either receptor may produce similar effects. Previous studies demonstrated that MDSC production of IL-10 is regulated by TLR4 (50). In the current report, the RAGE antagonist, A Box, partially restores T cell expression of L-selectin, suggesting that this effect of MDSC may be regulated through RAGE. The HMGB1 inhibitors ethyl pyruvate and glycyrrhizin reduced MDSC production of IL-10 during MDSC-macrophage crosstalk and the differentiation of MDSC from bone marrow progenitor cells, and ethyl pyruvate restored T cell activation in the presence of MDSC. These reagents either bind exogenous HMGB1 (glycyrrhizin) or inhibit NF-κB signaling (ethyl pyruvate) and therefore do not distinguish whether HMGB1 is acting through TLR4 or RAGE. Regardless of which receptor is utilized, HMGB1 is a potent inducer of MDSC and immune suppression, and both its pro-tumor and anti-tumor activities must be considered when designing cancer immunotherapies.

Supplementary Material

Refer to Web version on PubMed Central for supplementary material.

Acknowledgments

We thank Ms. Lisa Berkheimer for her excellent care of our mice, Ms. Julie Wolf for help with the cloning, Dr. James Thompson for generating the original shRNA irrelevant control construct, and Dr. Michael Lotze for providing the wild type and HMGB1-knock-out MEF cells.

Grant Support: This work was supported by NIH grants RO1CA115880, RO1CA84232 (SOR), and RO1GM098446 (HY). KP and LH were partially supported by US Department of Education grant P200A090094-11.

References

1. Gabrilovich DI, Bronte V, Chen SH, Colombo MP, Ochoa A, Ostrand-Rosenberg S, et al. The terminology issue for myeloid-derived suppressor cells. Cancer Res. 2007; 67:425. author reply 6. [PubMed: 17210725]
2. Gabrilovich DI, Nagaraj S. Myeloid-derived suppressor cells as regulators of the immune system. Nat Rev Immunol. 2009; 9:162–74. [PubMed: 19197294]
3. Sinha P, Clements VK, Bunt SK, Albelda SM, Ostrand-Rosenberg S. Cross-talk between myeloid-derived suppressor cells and macrophages subverts tumor immunity toward a type 2 response. J Immunol. 2007; 179:977–83. [PubMed: 17617589]
4. Hanson EM, Clements VK, Sinha P, Ilkovitch D, Ostrand-Rosenberg S. Myeloid-derived suppressor cells down-regulate L-selectin expression on CD4+ and CD8+ T cells. J Immunol. 2009; 183:937–44. [PubMed: 19553533]
5. Yang L, DeBusk LM, Fukuda K, Fingleton B, Green-Jarvis B, Shyr Y, et al. Expansion of myeloid immune suppressor Gr+CD11b+ cells in tumor-bearing host directly promotes tumor angiogenesis. Cancer Cell. 2004; 6:409–21. [PubMed: 15488763]

6. Yang L, Huang J, Ren X, Gorska AE, Chytil A, Aakre M, et al. Abrogation of TGF beta signaling in mammary carcinomas recruits Gr-1+CD11b+ myeloid cells that promote metastasis. Cancer Cell. 2008; 13:23–35. [PubMed: 18167337]
7. Balkwill F, Mantovani A. Inflammation and cancer: back to Virchow? Lancet. 2001; 357:539–45. [PubMed: 11229684]
8. Ostrand-Rosenberg S, Sinha P. Myeloid-derived suppressor cells: linking inflammation and cancer. J Immunol. 2009; 182:4499–506. [PubMed: 19342621]
9. Sims GP, Rowe DC, Rietdijk ST, Herbst R, Coyle AJ. HMGB1 and RAGE in inflammation and cancer. Annu Rev Immunol. 2010; 28:367–88. [PubMed: 20192808]
10. Lotze MT, Tracey KJ. High-mobility group box 1 protein (HMGB1): nuclear weapon in the immune arsenal. Nat Rev Immunol. 2005; 5:331–42. [PubMed: 15803152]
11. Wang H, Bloom O, Zhang M, Vishnubhakat JM, Ombrellino M, Che J, et al. HMG-1 as a late mediator of endotoxin lethality in mice. Science. 1999; 285:248–51. [PubMed: 10398600]
12. Li J, Kokkola R, Tabibzadeh S, Yang R, Ochani M, Qiang X, et al. Structural basis for the proinflammatory cytokine activity of high mobility group box 1. Mol Med. 2003; 9:37–45. [PubMed: 12765338]
13. Yang H, Tracey KJ. Targeting HMGB1 in inflammation. Biochim Biophys Acta. 2010; 1799:149–56. [PubMed: 19948257]
14. Yang H, Ochani M, Li J, Qiang X, Tanovic M, Harris HE, et al. Reversing established sepsis with antagonists of endogenous high-mobility group box 1. Proc Natl Acad Sci U S A. 2004; 101:296–301. [PubMed: 14695889]
15. Stewart TJ, Abrams SI. Altered immune function during long-term host-tumor interactions can be modulated to retard autochthonous neoplastic growth. J Immunol. 2007; 179:2851–9. [PubMed: 17709499]
16. Calogero S, Grassi F, Aguzzi A, Voigtlander T, Ferrier P, Ferrari S, et al. The lack of chromosomal protein Hmg1 does not disrupt cell growth but causes lethal hypoglycaemia in newborn mice. Nat Genet. 1999; 22:276–80. [PubMed: 10391216]
17. Sinha P, Clements VK, Ostrand-Rosenberg S. Reduction of myeloid-derived suppressor cells and induction of M1 macrophages facilitate the rejection of established metastatic disease. J Immunol. 2005; 174:636–45. [PubMed: 15634881]
18. Marigo I, Bosio E, Solito S, Mesa C, Fernandez A, Dolcetti L, et al. Tumor-induced tolerance and immune suppression depend on the C/EBPbeta transcription factor. Immunity. 2010; 32:790–802. [PubMed: 20605485]
19. Sinha P, Ostrand-Rosenberg S. Myeloid-derived suppressor cell function is reduced by Withaferin A, a potent and abundant component of Withania somnifera root extract. Cancer Immunol Immunother. 2013; 62:1663–73. [PubMed: 23982485]
20. Sinha P, Okoro C, Foell D, Freeze HH, Ostrand-Rosenberg S, Srikrishna G. Proinflammatory S100 proteins regulate the accumulation of myeloid-derived suppressor cells. J Immunol. 2008; 181:4666–75. [PubMed: 18802069]
21. Andersson U, Wang H, Palmblad K, Aveberger AC, Bloom O, Erlandsson-Harris H, et al. High mobility group 1 protein (HMG-1) stimulates proinflammatory cytokine synthesis in human monocytes. J Exp Med. 2000; 192:565–70. [PubMed: 10952726]
22. Park JS, Svetkauskaite D, He Q, Kim JY, Strassheim D, Ishizaka A, et al. Involvement of toll-like receptors 2 and 4 in cellular activation by high mobility group box 1 protein. J Biol Chem. 2004; 279:7370–7. [PubMed: 14660645]
23. Kokkola R, Andersson A, Mullins G, Ostberg T, Treutiger CJ, Arnold B, et al. RAGE is the major receptor for the proinflammatory activity of HMGB1 in rodent macrophages. Scand J Immunol. 2005; 61:1–9. [PubMed: 15644117]
24. Sinha P, Clements VK, Fulton AM, Ostrand-Rosenberg S. Prostaglandin E2 promotes tumor progression by inducing myeloid-derived suppressor cells. Cancer Res. 2007; 67:4507–13. [PubMed: 17483367]
25. Cheng P, Corzo CA, Luetteke N, Yu B, Nagaraj S, Bui MM, et al. Inhibition of dendritic cell differentiation and accumulation of myeloid-derived suppressor cells in cancer is regulated by S100A9 protein. J Exp Med. 2008; 205:2235–49. [PubMed: 18809714]

26. Ulloa L, Ochani M, Yang H, Tanovic M, Halperin D, Yang R, et al. Ethyl pyruvate prevents lethality in mice with established lethal sepsis and systemic inflammation. Proc Natl Acad Sci U S A. 2002; 99:12351–6. [PubMed: 12209006]
27. Yang H, Lundback P, Ottosson L, Erlandsson-Harris H, Venereau E, Bianchi ME, et al. Redox modification of cysteine residues regulates the cytokine activity of high mobility group box-1 (HMGB1). Mol Med. 2012; 18:250–9. [PubMed: 22105604]
28. Bianchi ME, Manfredi AA. High-mobility group box 1 (HMGB1) protein at the crossroads between innate and adaptive immunity. Immunol Rev. 2007; 220:35–46. [PubMed: 17979838]
29. Bronte V, Apolloni E, Cabrelle A, Ronca R, Serafini P, Zamboni P, et al. Identification of a CD11b(+)/Gr-1(+)/CD31(+) myeloid progenitor capable of activating or suppressing CD8(+) T cells. Blood. 2000; 96:3838–46. [PubMed: 11090068]
30. Gabrilovich DI, Velders MP, Sotomayor EM, Kast WM. Mechanism of immune dysfunction in cancer mediated by immature Gr-1+ myeloid cells. J Immunol. 2001; 166:5398–406. [PubMed: 11313376]
31. Kontgen F, Grumont RJ, Strasser A, Metcalf D, Li R, Tarlinton D, et al. Mice lacking the c-rel proto-oncogene exhibit defects in lymphocyte proliferation, humoral immunity, and interleukin-2 expression. Genes Dev. 1995; 9:1965–77. [PubMed: 7649478]
32. Huang B, Pan PY, Li Q, Sato AI, Levy DE, Bromberg J, et al. Gr-1+CD115+ Immature Myeloid Suppressor Cells Mediate the Development of Tumor-Induced T Regulatory Cells and T-Cell Anergy in Tumor-Bearing Host. Cancer Res. 2006; 66:1123–31. [PubMed: 16424049]
33. Bunt SK, Sinha P, Clements VK, Leips J, Ostrand-Rosenberg S. Inflammation induces myeloid-derived suppressor cells that facilitate tumor progression. J Immunol. 2006; 176:284–90. [PubMed: 16365420]
34. Bunt SK, Yang L, Sinha P, Clements VK, Leips J, Ostrand-Rosenberg S. Reduced inflammation in the tumor microenvironment delays the accumulation of myeloid-derived suppressor cells and limits tumor progression. Cancer Res. 2007; 67:10019–26. [PubMed: 17942936]
35. Pulaski BA, Ostrand-Rosenberg S. Reduction of established spontaneous mammary carcinoma metastases following immunotherapy with major histocompatibility complex class II and B7.1 cell-based tumor vaccines. Cancer Res. 1998; 58:1486–93. [PubMed: 9537252]
36. Liu Z, Falo LD Jr. You Z. Knockdown of HMGB1 in tumor cells attenuates their ability to induce regulatory T cells and uncovers naturally acquired CD8 T cell-dependent antitumor immunity. J Immunol. 2011; 187:118–25. [PubMed: 21642542]
37. Ellerman JE, Brown CK, de Vera M, Zeh HJ, Billiar T, Rubartelli A, et al. Masquerader: high mobility group box-1 and cancer. Clin Cancer Res. 2007; 13:2836–48. [PubMed: 17504981]
38. Song X, Krelin Y, Dvorkin T, Bjorkdahl O, Segal S, Dinarello CA, et al. CD11b+/Gr-1+ immature myeloid cells mediate suppression of T cells in mice bearing tumors of IL-1beta-secreting cells. J Immunol. 2005; 175:8200–8. [PubMed: 16339559]
39. Sha Y, Zmijewski J, Xu Z, Abraham E. HMGB1 develops enhanced proinflammatory activity by binding to cytokines. J Immunol. 2008; 180:2531–7. [PubMed: 18250463]
40. Liu JH, Li ZJ, Tang J, Liu YW, Zhao L, Deng P, et al. [High mobility group box-1 protein activates endothelial cells to produce cytokines and has synergistic effect with lipopolysaccharide in inducing interleukin-6 release]. Zhonghua Yi Xue Za Zhi. 2006; 86:1191–5. [PubMed: 16796861]
41. Leclerc P, Wahamaa H, Idborg H, Jakobsson PJ, Harris HE, Korotkova M. IL-1beta/HMGB1 complexes promote The PGE2 biosynthesis pathway in synovial fibroblasts. Scand J Immunol. 2013; 77:350–60. [PubMed: 23488692]
42. Rodriguez PC, Hernandez CP, Quiceno D, Dubinett SM, Zabaleta J, Ochoa JB, et al. Arginase I in myeloid suppressor cells is induced by COX-2 in lung carcinoma. J Exp Med. 2005; 202:931–9. [PubMed: 16186186]
43. Sade-Feldman M, Kanterman J, Ish-Shalom E, Elnekave M, Horwitz E, Baniyash M. Tumor necrosis factor-alpha blocks differentiation and enhances suppressive activity of immature myeloid cells during chronic inflammation. Immunity. 2013; 38:541–54. [PubMed: 23477736]

44. Wild CA, Bergmann C, Fritz G, Schuler P, Hoffmann TK, Lotfi R, et al. HMGB1 conveys immunosuppressive characteristics on regulatory and conventional T cells. Int Immunol. 2012; 24:485–94. [PubMed: 22473704]
45. Gebhardt C, Riehl A, Durchdewald M, Nemeth J, Furstenberger G, Muller-Decker K, et al. RAGE signaling sustains inflammation and promotes tumor development. J Exp Med. 2008; 205:275–85. [PubMed: 18208974]
46. Taguchi A, Blood DC, del Toro G, Canet A, Lee DC, Qu W, et al. Blockade of RAGE-amphoterin signalling suppresses tumour growth and metastases. Nature. 2000; 405:354–60. [PubMed: 10830965]
47. Livesey KM, Tang D, Zeh HJ, Lotze MT. Not just nuclear proteins: 'novel' autophagy cancer treatment targets - p53 and HMGB1. Curr Opin Investig Drugs. 2008; 9:1259–63.
48. Messmer D, Yang H, Telusma G, Knoll F, Li J, Messmer B, et al. High mobility group box protein 1: an endogenous signal for dendritic cell maturation and Th1 polarization. J Immunol. 2004; 173:307–13. [PubMed: 15210788]
49. Apetoh L, Ghiringhelli F, Tesniere A, Obeid M, Ortiz C, Criollo A, et al. Toll-like receptor 4-dependent contribution of the immune system to anticancer chemotherapy and radiotherapy. Nat Med. 2007; 13:1050–9. [PubMed: 17704786]
50. Bunt SK, Clements VK, Hanson EM, Sinha P, Ostrand-Rosenberg S. Inflammation enhances myeloid-derived suppressor cell cross-talk by signaling through Toll-like receptor 4. J Leukoc Biol. 2009; 85:996–1004. [PubMed: 19261929]
51. Coffelt SB, Scandurro AB. Tumors sound the alarmin(s). Cancer Res. 2008; 68:6482–5. [PubMed: 18701469]

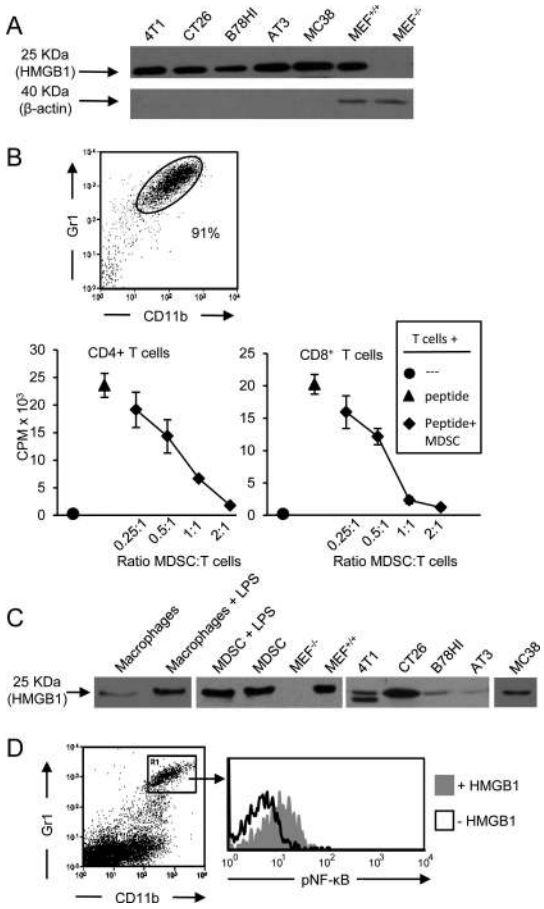

Figure 1. HMGB1 is ubiquitously present in the tumor microenvironment, is secreted by MDSC, and activates the NF-κB signaling pathway in MDSC

A, 4T1, CT26, B78H1, AT3 and MC38 tumor cells were cultured in serum-free medium and their supernatants assessed by western blot for secreted HMGB1. Lysates of wild type and HMGB1-knocked-out MEF cells served as positive and negative controls. ***B***, BALB/c 4T1-induced $Gr1^+CD11b^+$ MDSC were obtained from the blood of tumor-bearing mice, stained for Gr1 and CD11b to assess purity, and co-cultured with transgenic $CD4^+$ (DO11.10) or $CD8^+$ (clone4) splenocytes. Splenocytes were activated with OVA or HA peptide for DO11.10 and clone4 cells, respectively. T cell proliferation was measured by [^{3}H] thymidine incorporation. Data are expressed as cpm of triplicate cultures. ***C,*** LPS-treated and untreated macrophages and MDSC, and excised, dissociated tumors of BALB/c (4T1, CT26) and C57BL/6 (B78HI, AT3, MC38) mice were cultured overnight in serum-free medium. Resulting supernatants were assessed by western blot for HMGB1. ***D,*** Leukocytes from tumor-free BALB/c mice were treated with or without HMGB1 and stained for Gr1, CD11b, and pNF-κB. $Gr1^+CD11b^+$ cells were gated and analyzed for pNF-κB. Data are from one of three, two, three, and three independent experiments for panels A, B, C, and D, respectively.

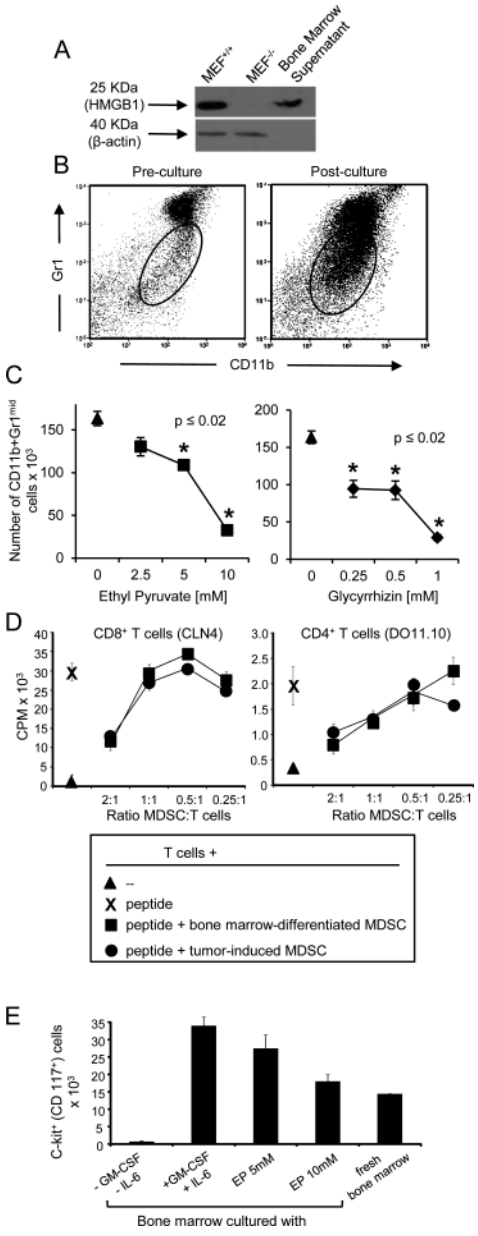

Figure 2. HMGB1 drives the differentiation of MDSC from bone marrow progenitor cells

Bone marrow cells were harvested from the femurs of healthy BALB/c mice and cultured with IL-6 and GM-CSF with or without ethyl pyruvate, glycyrrhizin, or vehicle. After four days of culture, the absolute number of MDSC was determined. ***A,*** HMGB1 western blot of supernatants of bone marrow cultures. ***B***, Gating logic of $Gr1^{mid}CD11b^{+}$ MDSC from pre-cultured and post-cultured bone marrow cells. ***C,*** Absolute number of $Gr1^{mid}CD11b^{+}$ MDSC in the bone marrow cultures after incubation with ethyl pyruvate or glycyrrhizin. ***D,*** MDSC generated in the bone marrow cultures were assessed for suppressive activity against antigen-specific MHC-restricted transgenic $CD4^{+}$ and $CD8^{+}$ T cells. ***E,*** Bone marrow cells were cultured under MDSC differentiation conditions (GM-CSF+IL-6) ± ethyl pyruvate (EP) and analyzed for the percent of c-kit^{+} ($CD117^{+}$) progenitor cells. p values were

obtained by Student's *t* test. Data are from one of three and two independent experiments for panels A-C and D-E, respectively.

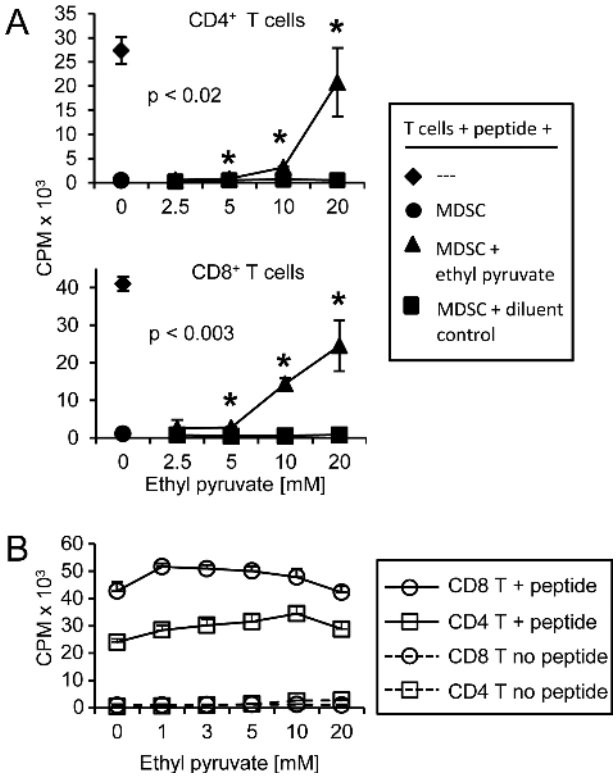

Figure 3. HMGB1 contributes to the ability of MDSC to suppress antigen-driven T cell activation

Splenocytes from CD4+ DO11.10 TcR or CD8+ clone4 TcR transgenic mice were co-cultured with irradiated 4T1-induced MDSC from BALB/c mice and cognate peptide (OVA or HA peptide for DO11.10 and clone 4 T cells, respectively). ***A***, T cell proliferation was measured by [^{3}H]-thymidine incorporation in the presence of titered amounts of ethyl pyruvate or vehicle control. ***B***, Ethyl pyruvate does not directly affect T cell activation. Transgenic DO11.10 and clone4 T cells were activated with cognate peptide in the presence of titered amounts of ethyl pyruvate. Data are from one of two independent experiments. p values were obtained by Student's *t* test comparing ethyl pyruvate treated samples versus the respective diluent control samples.

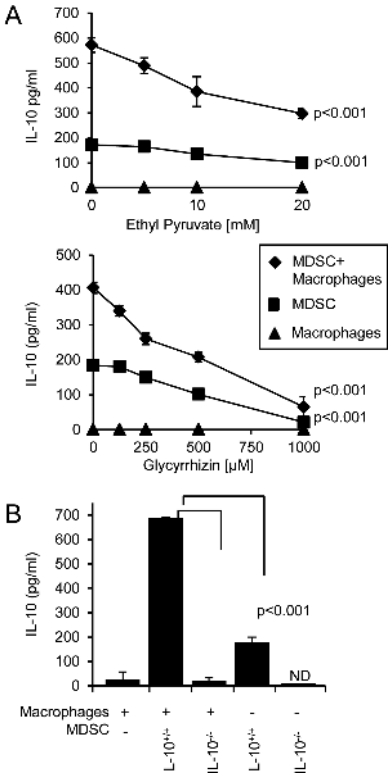

Figure 4. HMGB1 increases MDSC production of IL-10 and MDSC-macrophage crosstalk

A, Co-cultures of 4T1-induced BALB/c MDSC and macrophages from tumor-free mice were incubated with or without ethyl pyruvate or glycyrrhizin, and the supernatants were assayed by ELISA for IL-10. ***B,*** MDSC from 4T1-tumor-bearing BALB/c and BALB/c IL-$10^{-/-}$ mice and peritoneal macrophages from tumor-free BALB/c mice were co-cultured and the supernatants were assayed by ELISA for IL-10. ND indicates non-detectable levels of protein. Data are from one of six and three independent experiments for panels A and B, respectively. p values were obtained by single-factor ANOVA.

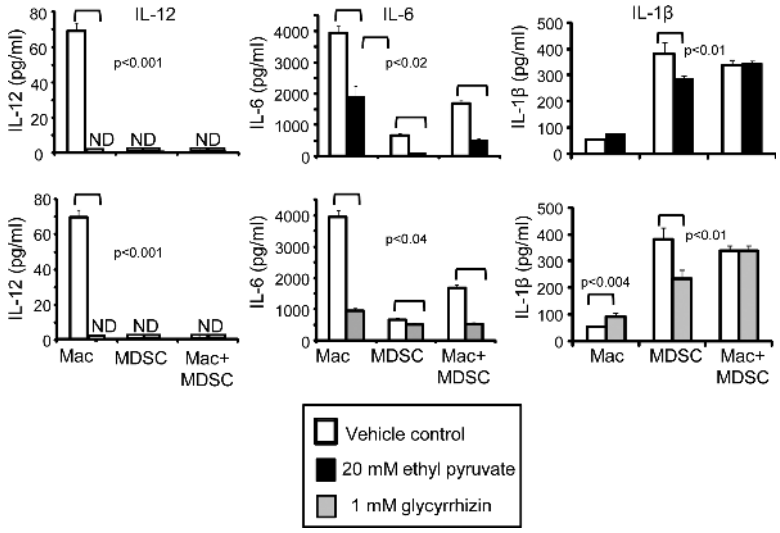

Figure 5. HMGB1 facilitates down-regulation of IL-6 and MDSC production of IL-1β, but does not alter MDSC-mediated down-regulation of macrophage production of IL-12

Co-cultures of 4T1-induced BALB/c MDSC and macrophages from tumor-free mice were incubated with or without ethyl pyruvate or glycyrrhizin and the supernatants were assayed by ELISA for IL-12, IL-6, and IL-1β. ND indicates non-detectable levels of protein. Data are from one of four, five, and two independent experiments for IL-12, IL-6, and IL-1β, respectively. p values were obtained by Student's *t* test.

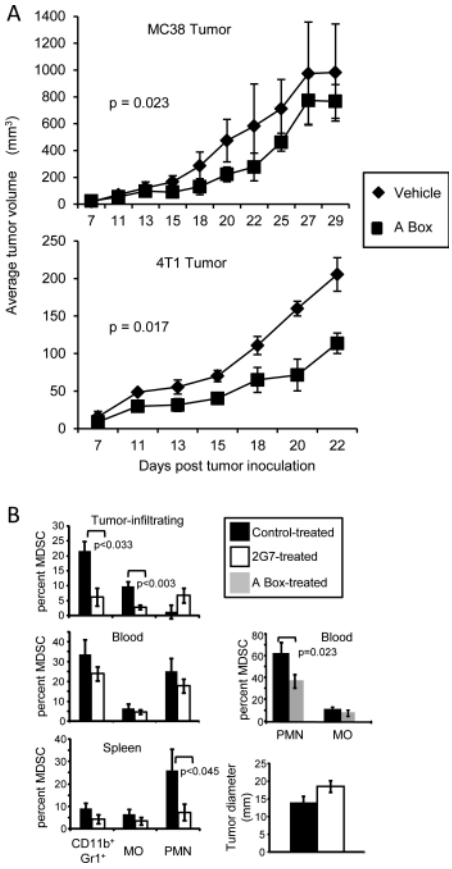

Figure 6. Tumor-bearing mice treated with mAbs to HMGB1 or with A Box have reduced levels of MDSC

A, C57BL/6 and BALB/c mice were inoculated s.c. with 5 x 10^5 MC38 colon carcinoma cells or in the mammary fat pad with 7 x 10^3 4T1 mammary carcinoma cells, respectively. Mice were given recombinant A box (300μg/mouse) or vehicle (PBS) three times per week starting when tumors were first palpable (day 7-9 post inoculation). p values were obtained by log rank test. ***B,*** C57BL/6 mice were inoculated as in panel A. Treatment with 2G7 (5μg/200μl/mouse, 3x/week), irrelevant IgG, or A Box was started on day 10-13 when tumors were first palpable. Treatment was terminated on day 45 and blood leukocytes were analyzed by flow cytometry for total ($Gr1^+CD11b^+$), monocytic (MO; $CD11b^+Ly6G^-Ly6C^+$), and granulocytic (PMN; $CD11b^+Ly6G^+Ly6C^-$) MDSC. Mice were sacrificed on day 50 when their tumors were approximately the same size, and spleen and tumor-infiltrating leukocytes ($CD45^+$ cells) were analyzed by flow cytometry. n = 7 (blood, control-treated for 2G7), 4 (A Box, PBS-treated), 6 (tumor-infiltrating and spleen, control-treated; blood, 2G7-treated), 4 (tumor-infiltrating and spleen, 2G7-treated), and 4 (A Box-treated) mice/group. Data for 2G7 and their control-treated mice are pooled from two independent experiments; data for A Box and their control-treated mice are from a single experiment.

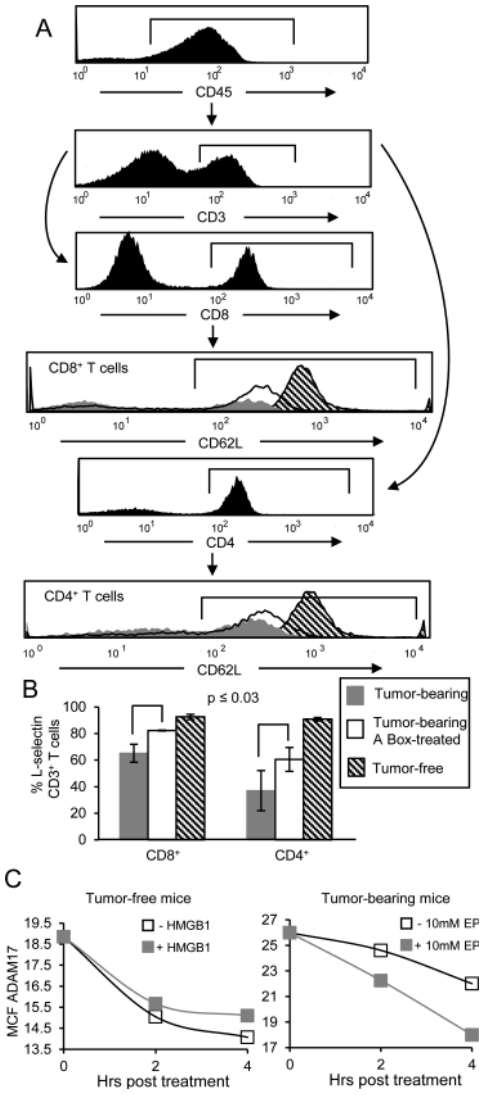

Figure 7. HMGB1 down-regulates T cell expression of L-selectin

A, Twenty-nine days after tumor inoculation the MC38 tumor-bearing mice from figure 6A were sacrificed and blood leukocytes were analyzed by flow cytometry for L-selectin expression and compared to blood leukocytes from tumor-free C57BL/6 mice. Representative histograms showing L-selectin expression from gated $CD45^+CD3^+CD4^+$ and $CD45^+CD3^+CD8^+$ T cells from tumor-free, A box-treated, or control-treated (PBS) C56BL/6 tumor-bearing mice. ***B,*** Average percent ± SD of $CD45^+CD3^+CD4^+$ or $CD45^+CD3^+CD8^+$ T cells expressing L-selectin. n= 5 mice/group (PBS-treated and tumor-free groups); n= 3 mice/group (A Box-treated group). p values were obtained by Student's *t* test. Data are from one of two independent experiments. ***C,*** $Gr1^+CD11b^+$ cells from tumor-free (left-hand panels) or tumor-bearing (right-hand panels) mice were incubated in vitro for zero, two, or four 4 hours with exogenous HMGB1 (left-hand panels) or ethyl pyruvate (right-hand panels), and stained for Gr1, CD11b, and ADAM17. Gated $Gr1^+CD11b^+$ cells

were analyzed for ADAM17 expression. Graphs represent MCF of ADAM17 on $Gr1^{+}CD11b^{+}$ cells. Data are representative of three independent experiments.